Geological Quarterly, 2002, **46** (4): 449–461

Identification of Miocene gas deposits from seismic data in the southeastern part of the Carpathian Foredeep

Kaja PIETSCH and Jadwiga JARZYNA

Pietsch K. and Jarzyna J. (2002) — Identification of Miocene gas deposits from seismic data in the southeastern part of the Carpathian Foredeep. Geol. Quart., **46** (4): 449–461. Warszawa.

Seismic interpretations are normally made to help identify and locate structural and stratigraphic traps for oil. We focus on problems in interpreting seismic sections in sandy-shaly Miocene deposits which occur in the eastern part of the Polish Carpathian Foredeep. There, the structural picture yielded by the seismic section is not in good agreement with the known structure and a correct interpretation of the seismic wave field, based on seismic modelling, is needed to ensure proper location of exploratory and production wells. We show that the correct choice of petrophysical parameters in these deposits allows interpretation of the seismic image in terms of a multi-horizon gas body. A decrease in velocity, characteristic of gas-saturated beds, was not observed in velocity obtained from sonic measurements. Therefore, several versions of a seismogeological model were constructed based on the results of integrated log interpretation. A model using seismic wave velocity obtained from acoustic wave velocity and a quality factor Q, as a measure of attenuation of elastic waves, was of particular significance. In addition to the petrophysical parameters, the strata geometry necessary to construct a seismogeological model, was determined. Combining the interpreted geometry and information regarding depths of lithostratigraphic units an anticlinal structure was deduced in the gas-rich zone. A comparison of synthetic seismograms calculated using only sonic velocity and seismic velocity corrected for attenuation, with the recorded seismic traces, shows that the best agreement was obtained for a model which included the attenuation. Differences observed between the synthetic and field sections were a basis for determining local direct hydrocarbon indicators, which were then used to identify hydrocarbon deposits in the recorded seismic section.

Kaja Pietsch, Jadwiga Jarzyna, Department of Geophysics, Faculty of Geology, Geophysics and Environmental Protection, University of Mining and Metallurgy, Mickiewicza 30, PL-30-059 Kraków, Poland, e-mails: pietsch@geolog.geol.agh.edu.pl; jarzyna@geol.agh.edu.pl *(received: July 23, 2001; accepted: May 8, 2002).*

Key words: Carpathian Foredeep, seismics, seismostratigraphy, velocity model, acoustic full wavetrain, attenuation of seismic waves.

INTRODUCTION

The role of seismics in oil and gas prospecting has long been acknowledged. Seismic surveys may give direct indications of hydrocarbons via the dependence of velocity and attenuation of P-waves and S-waves on oil and gas saturation in the pore space. Eventually, as a result of seismic interpretation, structural and stratigraphic traps may be successfully identified and located. Some problems with interpretation of seismic data in gas fields may occur because elastic wave velocity is significantly lower in gas-saturated horizons thus resulting in:

— sag of seismic horizons beneath a deposit what may give rise to unreal positive undulations beyond the deposit;

— bright spot events due to an increase in the absolute value of the reflection coefficient.

Difficulties with the unequivocal interpretation of seismic data occur, when a seismic section does not reflect the structural arrangement of layers, for instance in multi-horizon gas fields. Since the petrophysical parameters of a hydrocarbon-saturated rock medium may be variable, and the same causes may produce different effects, there is a need to determine the so-called direct hydrocarbon indicators (Dilay, 1982; Blackburn, 1986; Sheriff, 1992).

There have been problems in the identification of small structural and stratigraphic traps in sandy-shaly Miocene deposits in the eastern part of the Polish Carpathian Foredeep. In this area, the structural picture yielded by the seismic profiles does not often agree with the structure as deduced by other means (Borys *et al*., 1999). Hence, correct geological interpretations of the seismic wave field, based on 1D and 2D seismic modelling, are needed for the proper location of exploratory and production wells (Pietsch *et al*., 1998).

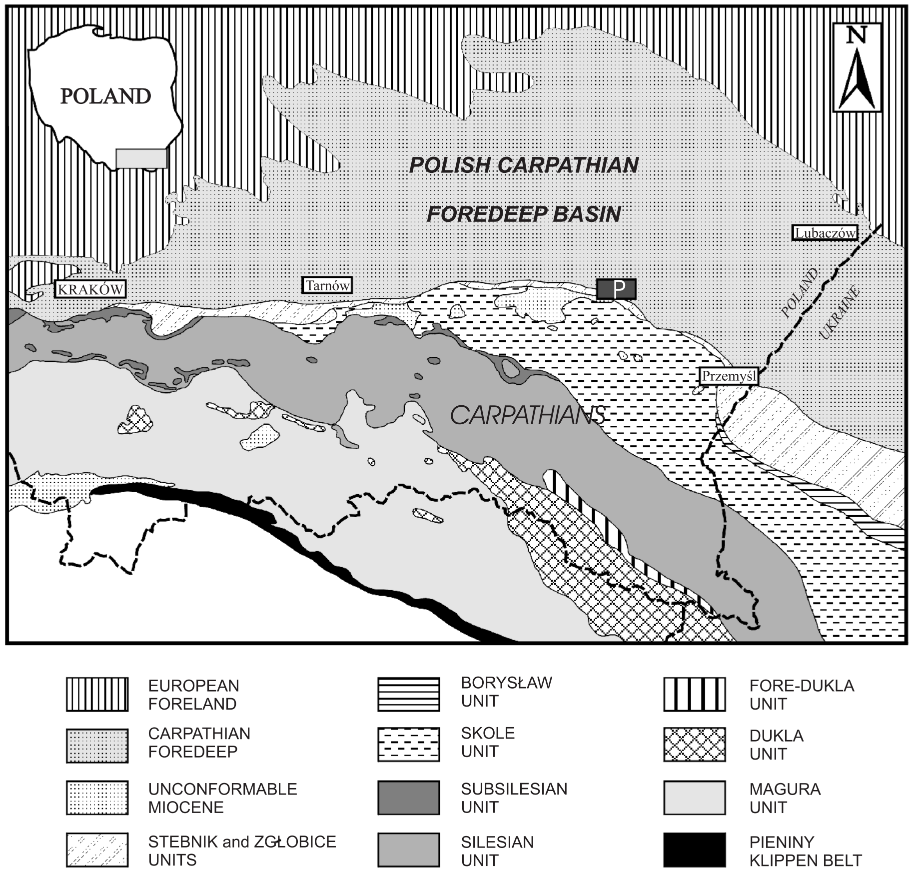

Fig. 1. Map showing the location of the gas field P and rock units in the Carpathians and the Carpathian Foredeep (after Krzywiec, 2001)

Table 1

Results of interpretation of well logs and inflow measurements in borehole P-6

No. of gas horizon	Depth of packer investigation [m]	PHI [%]	SW [%]	RHOB [g/ccm]	V_SONIC [m/s]	GR [API]	Q	V_Q [m/s]	Inflow [Nm^3/min]
1	1304–1314	7.01	99.35	2.38	3277	73.28	15	2961	280
2	1347–1383	4.27	99.94	2.43	3274	79.18	18	2847	83
3	1430–1437	2.04	99.97	2.49	3174	86.51	19	2795	74
4	1468–1486	6.98	97.07	2.37	3255	68.96	5	2054	323
5	1585–1595	4.3	98.67	2.46	3331	78.91	16	2819	104
6	1667–1692	3.33	98.72	2.54	3253	81.48	19	2861	70
7	2150–2195	1.59	99.52	2.58	3790	92.53	24	3394	25

The comprehensive interpretation of seismic data should include:

— construction of seismogeological models of reservoir zones,

— modelling of theoretical seismic wave field given in the form of 1D synthetic seismograms and 2D synthetic seismic profiles,

— identification of gas-induced anomalies observed in the theoretical wave field,

— determination of reservoir parameters from seismic data based on criteria for direct hydrocarbon indicators.

GEOLOGICAL SETTING

The Carpathian Foredeep Basin in SE Poland originated during the Miocene as a result of flexural subsidence in the

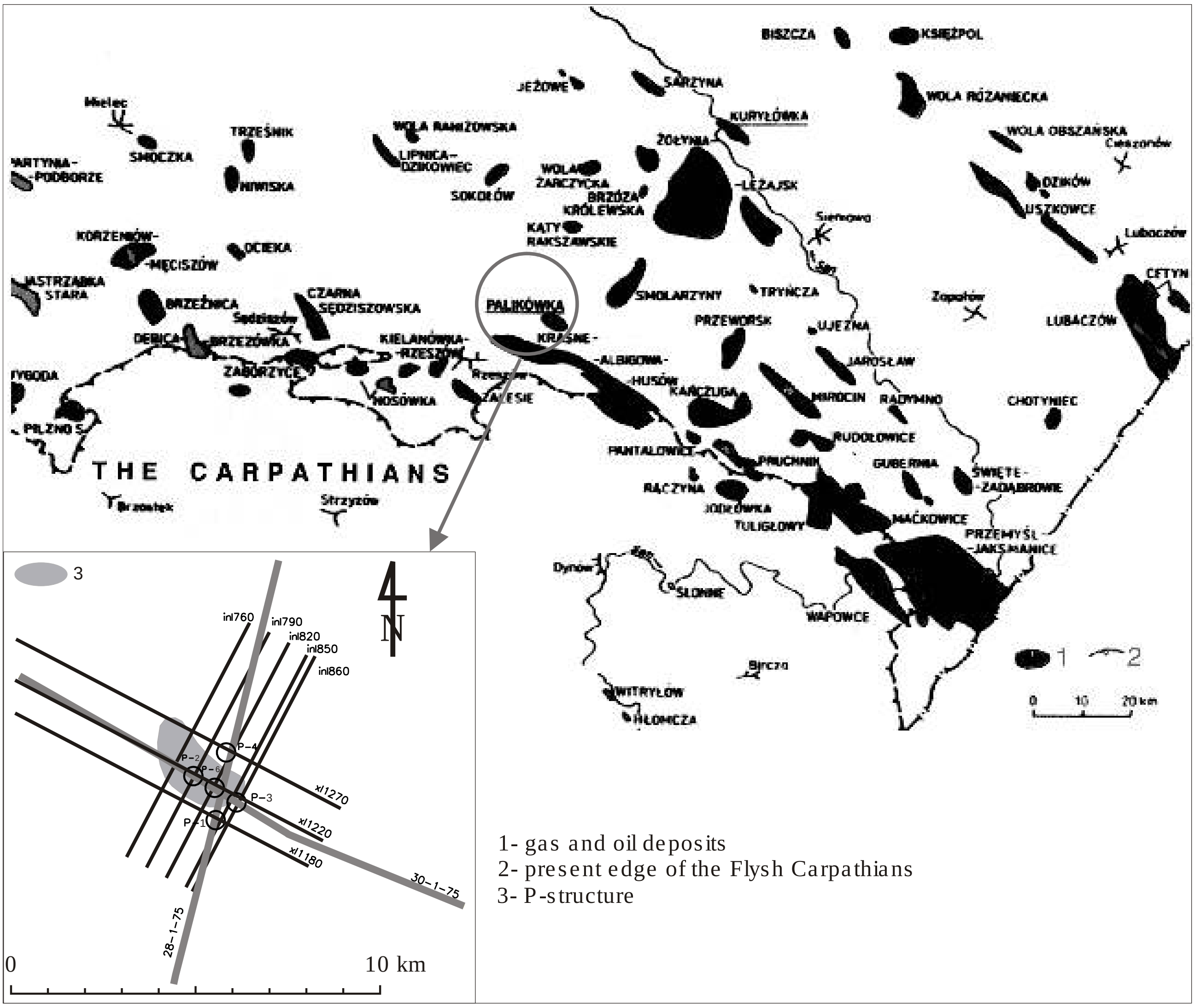

Fig. 2. Location of the gas field P with seismic profiles and wells, against a context of other hydrocarbon deposits in the SE part of the Carpathian Foredeep (after Karnkowski, 1999)

30-1-75 and 28-1-75 — 2D seismic lines; inl760, inl790, inl820, inl850, inl860, xl 1270, xl 1220, xl 180 — 3D seismic lines

front of flysch nappes that were thrust northwards onto the East European Platform. Near its southern, active margin the basin was filled with 2000–3000 m of mainly siliciclastic deposits of submarine-fan, slope, and deltaic facies. To the south, part of the succession was removed due to tectonic uplift on the frontal Carpathian overthrust that forms a major seal for the most hydrocarbon accumulations in the Carpathian Foredeep in Poland (Stupnicka, 1989; Krzywiec, 2001) (Fig. 1).

The width of the outer foredeep (outside of the Carpathians) varies between 30–40 km in the western segment up to 90 km in the eastern one. The outer foredeep is filled with Badenian and Sarmatian marine deposits, from few hundred up to about 3500 m in thickness (Oszczypko, 1996).

Evaporites constitute the main correlation level in the Carpathian Foredeep. Traditionally, the Badenian deposits are divided into lower (sub-evaporatic), middle (evaporatic) and upper (supra-evaporatic) units. We employ this division, though a more recent chronostratigraphical subdivision foredeep sediments has been made (Steininger *et al*., 1990 in Oszczypko, 1996).

In the study area, the Miocene succession is >2000 m thick and rests unconformably on Upper Precambrian basement. The succession begins with the lower Badenian Baranów Beds, which are overlain by middle Badenian anhydrites. The upper Badenian consists of mudstones and shales intercalated with very thin layers of fine-grained sandstones. The overlying Sarmatian deposits are developed as fine- to coarse-grained sandstones and shales, which exhibit strong facies variability. The sandstones, locally up to 150 m in thickness, dominate in the lower part of the Sarmatian, while claystones and mudstones increase in abundance towards its top. There are many small hydrocarbon deposits in the Sarmatian rocks (Fig. 2) (Karnkowski, 1999).

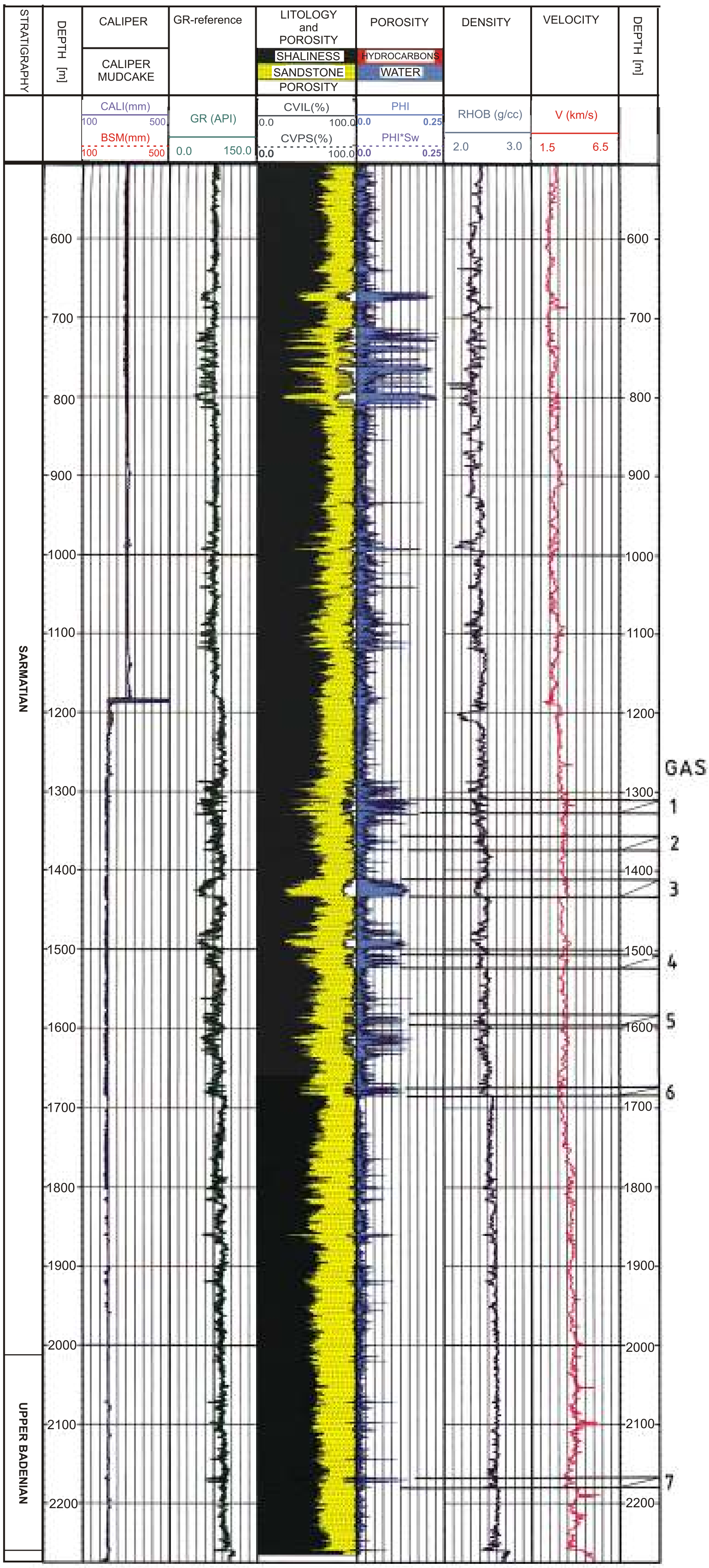

Fig. 3. Interpretation results of borehole P-6 (made by Geofizyka Kraków Ltd.)

PHI — porosity, SW — water saturation, GR — intensity of natural radioactivity, CAL — real diameter of borehole, RHOB — bulk density, V — velocity

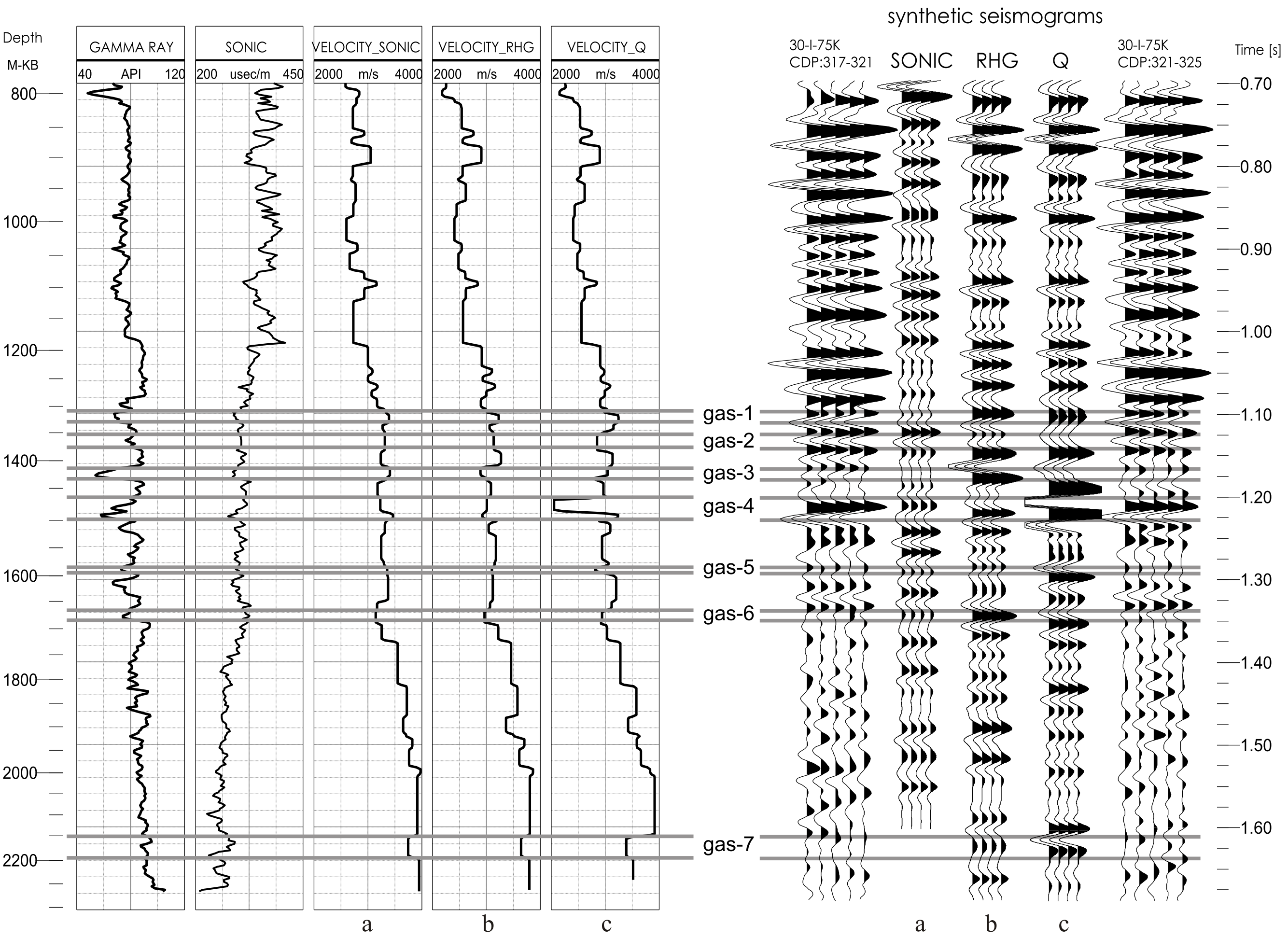

Fig. 4. Comparison of GR and sonic curves with modeled velocities and corresponding synthetic seismograms

a — VELOCITY_SONIC, b — VELOCITY_RHG, c — VELOCITY_Q; 1–7 — gas horizons

SEISMOGEOLOGICAL MODEL

A seismogeological model of the gas field P, needed for construction of the theoretical seismic section, was made using interpretation results for 2D and 3D seismic profiles and well logs from the study area (Fig. 2). Interpretation of 2D and 3D seismic sections, made on a CHARISMA-GeoFrame 3.8.1 (*Schlumberger GeoQuest*), gave the geometry of seismic boundaries, which corresponded to layers with varied lithology and different reservoir parameters: porosity and gas saturation.

In structure P, located over a small structural elevation of the basement recognised by the seismic survey, several wells were drilled: P-1, P-2, P-3, P-4, P-5 and P-6. These were all logged. Sonic logs were made in the non-productive borehole P-4 and in the productive borehole P-6. The results of comprehensive interpretations of well logs in the boreholes were combined with the seismic results to recognise the mutual relations between the reservoir parameters of layers, the seismic model and the geological model.

WELL LOG DATA

A correct selection of petrophysical parameters of layers of a seismogeological model is of great importance to that part of the Carpathian Foredeep. There, a decrease in velocity, as is characteristic of gas beds, was not observed in velocity curves obtained from sonic measurements (Pietsch *et al.*, 1998; Bała, 2001). Therefore, in this study three seismogeological models were constructed based on the results of integrated interpretation of logs from wells P-6 and P-4. Quantitative interpretation of well logs was made by Geofizyka Kraków Ltd. Interpretation results for the 0–2280 m depth interval of borehole P-6 in terms of lithology–porosity–saturation curves are shown in Figure 3. The amount of sandstones and shales changes little in the study profile. Gas saturation was observed in a few levels of increased porosity. The volume of the inflow was determined from packer measurements. Results of log interpretations of the gas bearing horizons in terms of porosity — PHI, water saturation — SW, and quality factor — Q, as a measure of attenuation, together with values of bulk density — RHOB, natural radioactivity —

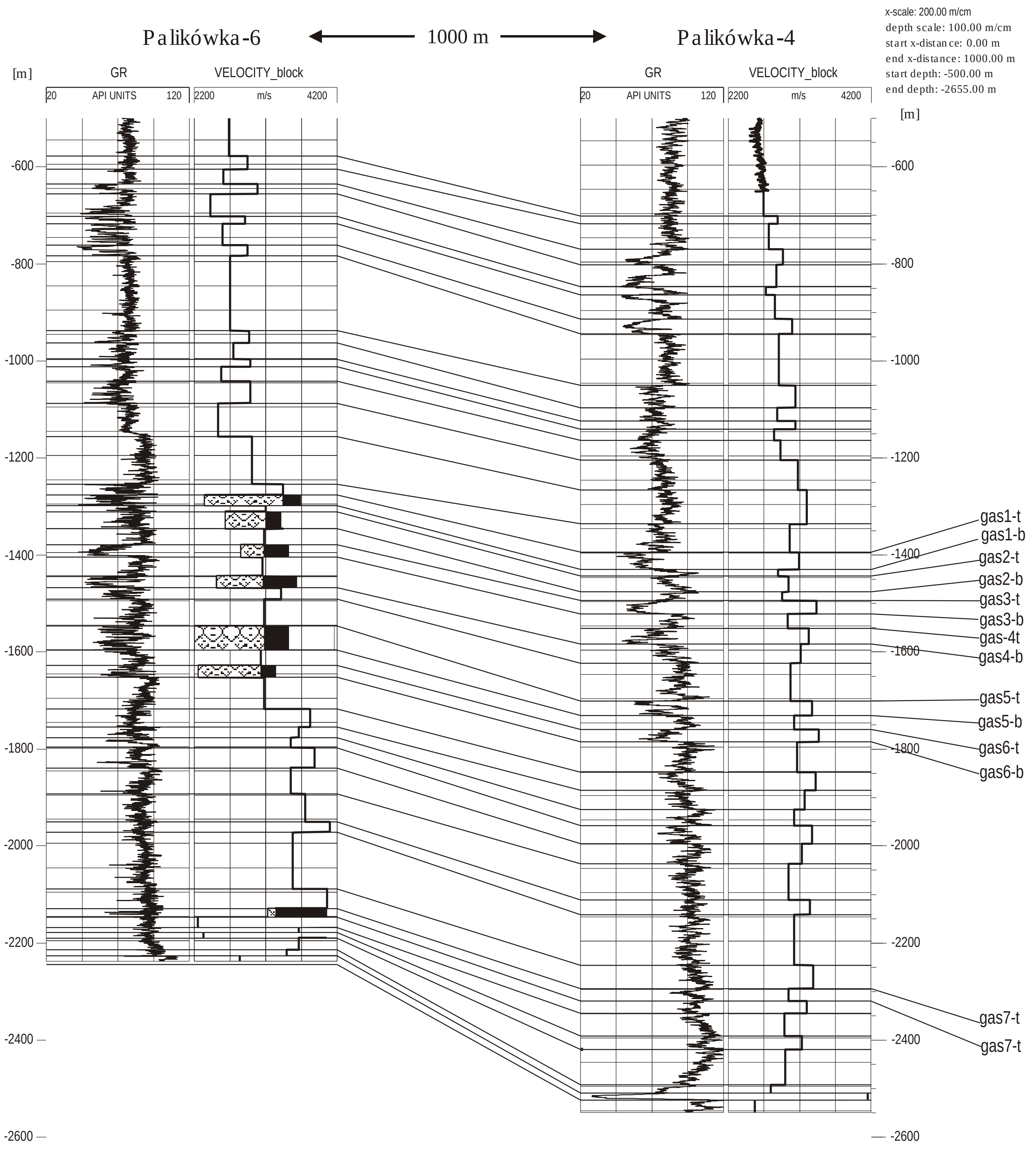

Fig. 5. Correlation of Miocene horizons in wells P-6 and P-4, gas field P

GR, sonic velocity — V_SONIC, seismic velocity — V_Q, for selected horizons are shown in Table 1.

VELOCITY FROM LOGS

Horizon velocity (VELOCITY_SONIC) was determined for layers distinguished based on a VSP-corrected sonic curve and lithological interpretation. Gas-saturated layers (horizons 1 –7 in Table 1 and in Fig. 4) correlate with the GR (low amplitude) and porosity (high amplitude). However, there is no clear relation between anomalies in the velocity curve from the sonic log and from the location of gas layers. The shape of the sonic curve is a result of the shallow radius of investigation of the sonic log in a flushed zone, where pore space was saturated with a mud filtrate, and gas was thus removed from the vicinity of the borehole walls, causing a decrease in transit interval time. Therefore, the expected decrease of velocity (increase of

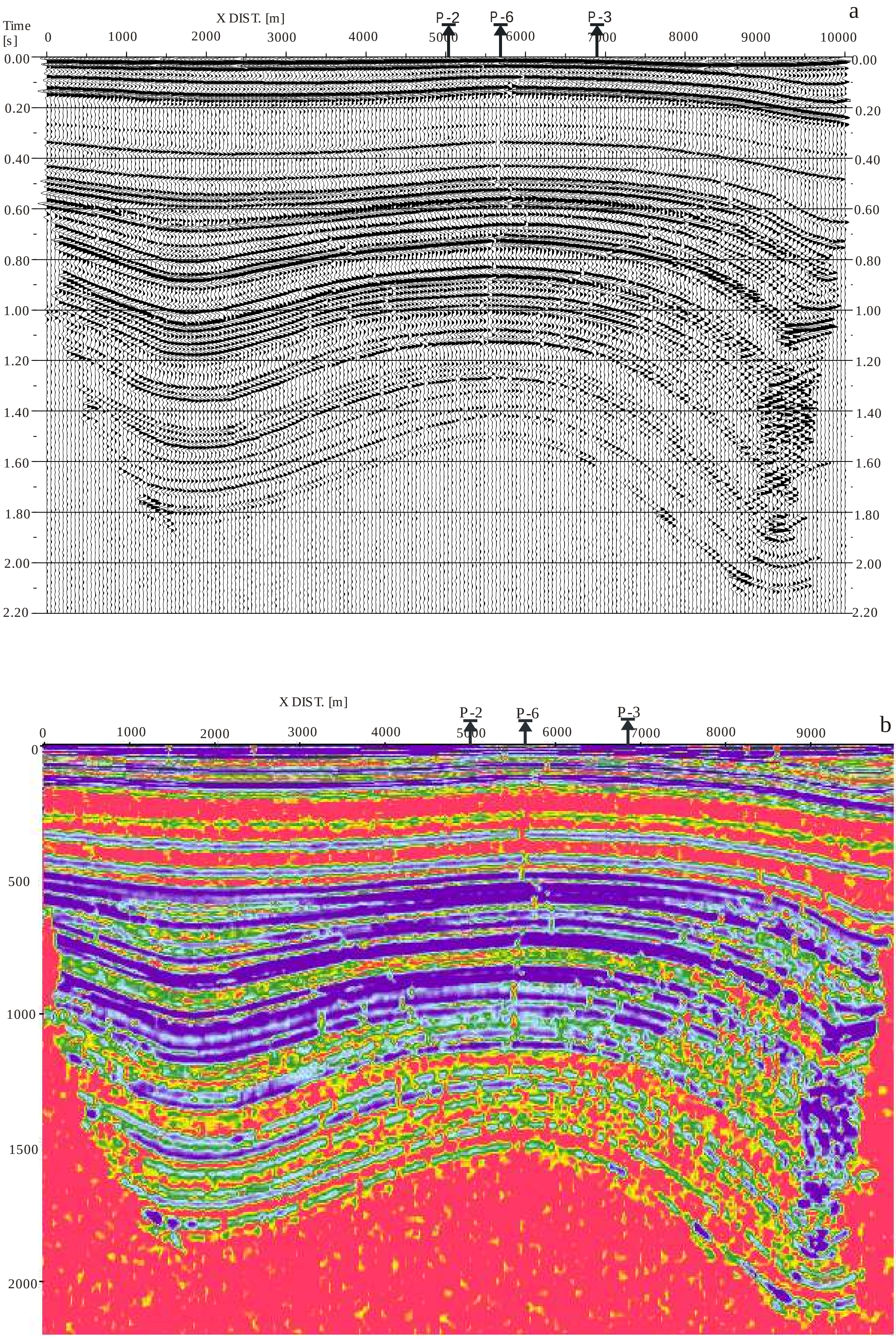

Fig. 6. Theoretical seismic section, model “without gas”

a — NORMAL INCIDENCE, b — REFLECTION STRENGTH

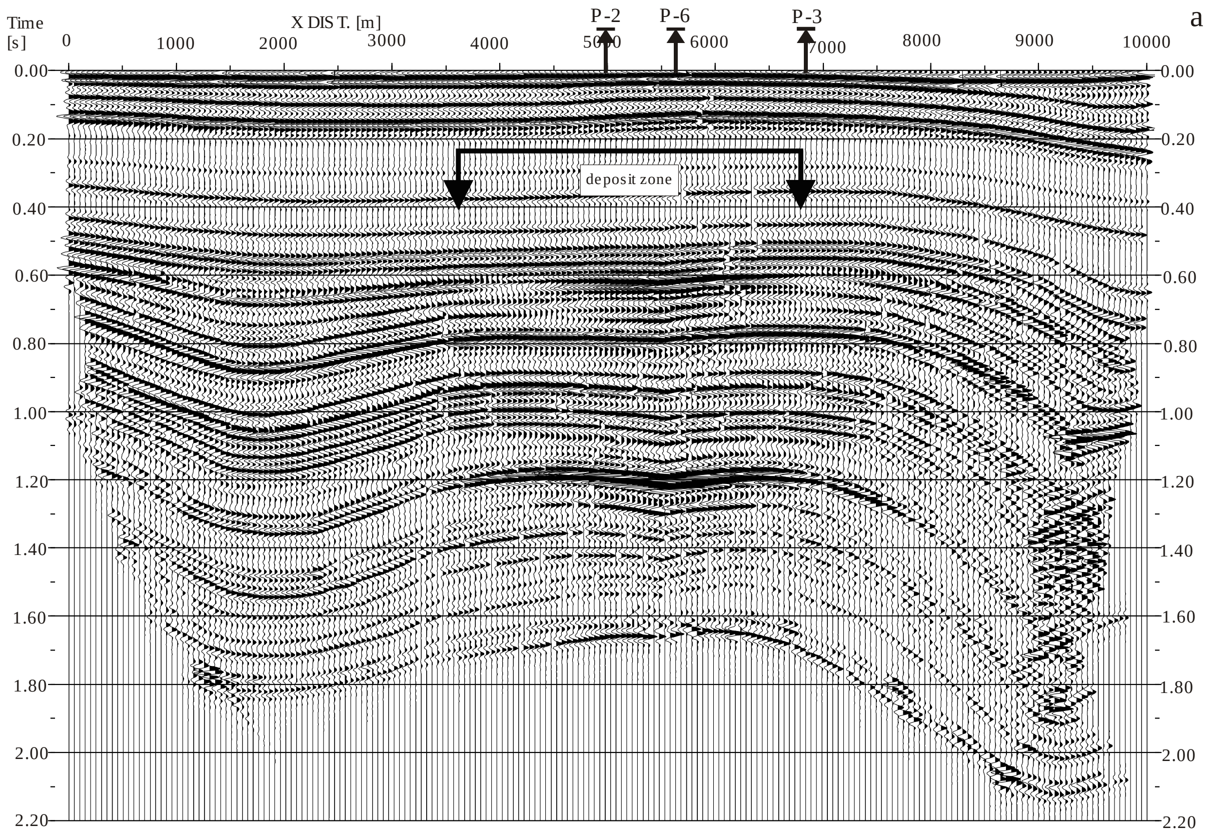
a
Time [s]
X DIST. [m]
0 1000 2000 3000 4000 5000 6000 7000 8000 9000 10000
P-2
P-6
P-3
deposit zone
0.00 0.20 0.40 0.60 0.80 1.00 1.20 1.40 1.60 1.80 2.00 2.20

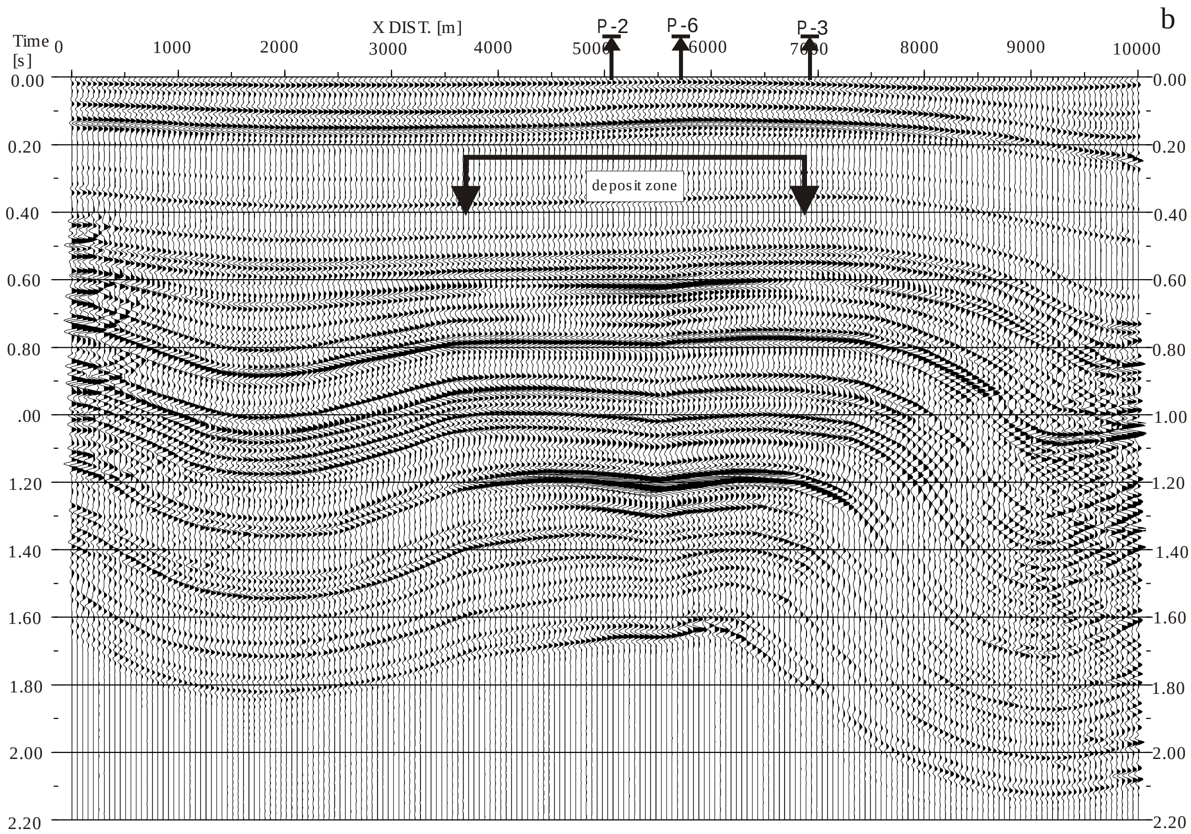
b
Time [s]
X DIST. [m]
0 1000 2000 3000 4000 5000 6000 7000 8000 9000 10000
P-2
P-6
P-3
deposit zone
0.00 0.20 0.40 0.60 0.80 .00 1.20 1.40 1.60 1.80 2.00 2.20

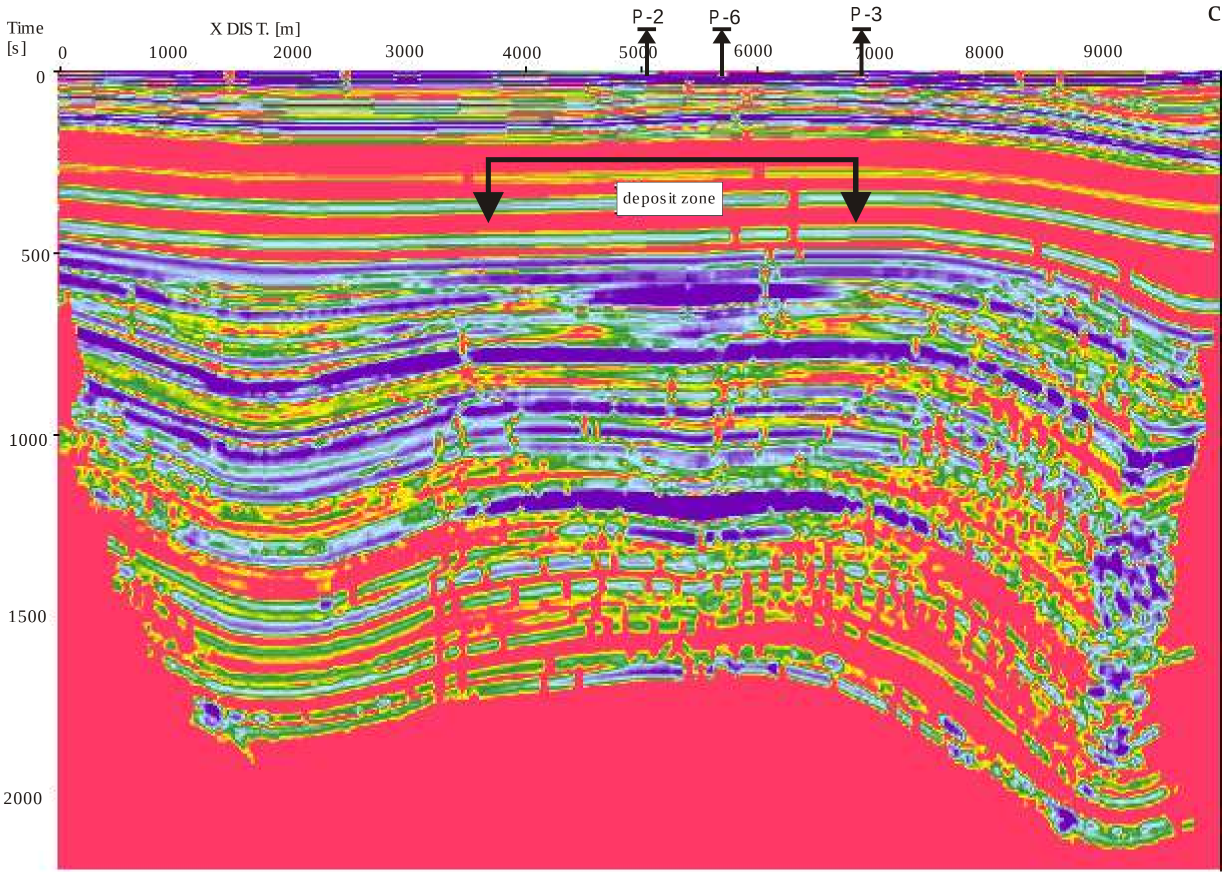

Fig. 7. Theoretical seismic section, model "with gas"

a — NORMAL, b — DIFFRACTION + STOLT MIGRATION, c — NORMAL-REFLECTION STRENGTH

transit interval time) associated with the gas horizons was not observed (Pietsch *et al*., 1998).

In the second case, a velocity (VELOCITY_RHG) was calculated using the Raymer-Hunt-Gardner equation (Raymer *et al*., 1980) and compared with the VELOCITY_SONIC. In some horizons the decrease in VELOCITY_RHG reaches as much as 20%. A decrease in VELOCITY_RHG and increase in VELOCITY_SONIC was observed for all gas horizons except for horizon 7. Such discrepancy between both velocities (greater for higher porosity) was not observed in non-gas horizons with higher porosity. An exception was the horizon at a 675–825 m depth in which packer measurements were not made. There, both velocities behave as in deposit zones.

A third velocity model (VELOCITY_Q) was obtained from the sonic log with the quality factor, Q, included (Aki and Richards, 1980). The comparison of VELOCITY_Q with two others shows the significant role of this result in the interpretation.

Quality factor was used here as a measure of attenuation of seismic waves. Knowledge of the attenuation and thus the connection of lithological and seismic parameters is fundamental in lithological and reservoir interpretation of seismic data (Stewart *et al*., 1984). Various authors have attempted estimation of P-wave attenuation from VSP and acoustic full wavetrains (Hardage, 1985; Toverund and Ursin, 1998). One of the most popular and effective methods for obtaining the Q factor, basing on the logarithmic spectral ratio, was employed in this paper (De *et al*., 1994).

The interpretation of selected pairs of acoustic full wavetrains recorded with an LSS device (Halliburton) was made for several boreholes to determine the quality factor, Q, for Miocene shaly-sandy rocks (Jarzyna, 1999). The basic difficulty in obtaining correct values of quality factor in this case was the limited number of wavetrains with amplitudes satisfying assumptions for the amplitude spectra ratio method (Bała and Jarzyna, 1992). Thus, values of the quality factor, Q, should be treated as low-confidence estimates of attenuation.

The three above-defined velocities were compared with petrophysical parameter curves in well P-6. The best

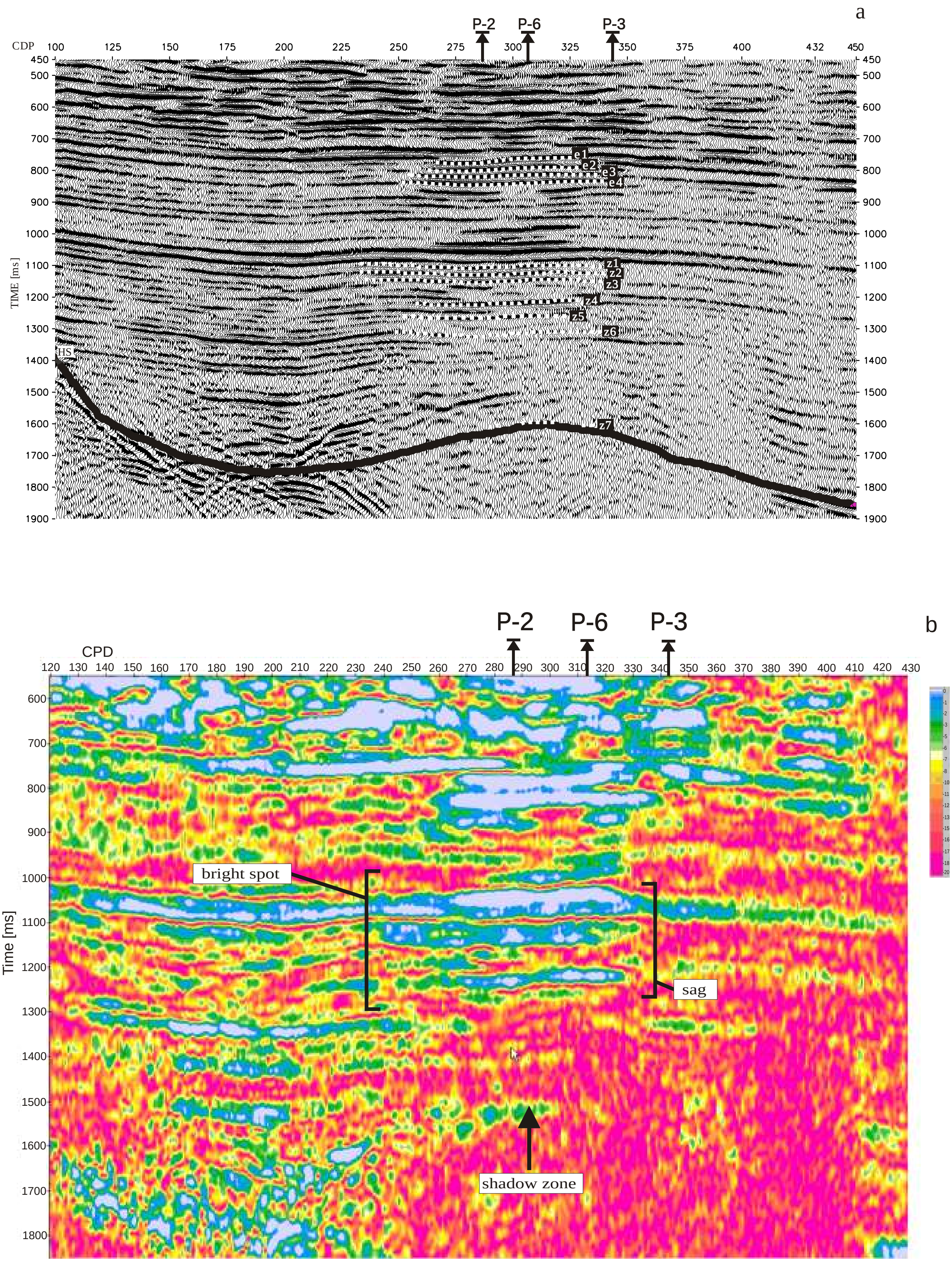

Fig. 8. Results of interpretation for 30-I-75K line made on the CHARISMA system for the deposit P

a — seismic section; marked confirmed gas horizons (z1-z7) in the lower part and probable gas horizons (e1-e4) in the upper part the seismic section, HS – top of basement, b — reflection strength correspondence was observed between VELOCITY_Q and GR and porosity and inflow values.

SEISMIC MODEL — GEOMETRICAL ARRANGEMENT

The geometric arrangement of boundaries in the seismogeological model was assumed on the basis of the interpretation of the seismic profile 30-1-75K. The time-depth conversion and geological correspondence of seismic layers was determined using velocity curves and synthetic seismograms calculated for wells P-6 and P-4. The results of this interpretation were used to determine the geometry of seismic boundaries outside the structural elevation in the basement, the P-structure, in which the deposit is located. In the P-structure itself, an anticlinal geometry of strata was assumed, corresponding to the structural plan of the basement, even though it was not visible on the seismic image. The width of the deposit zone was adopted from interpretation of well logs in well P-2 (productive) and in well P-3 (non-productive) as well as from preliminary interpretation of seismic profiles (location of anticlinal arrangement of basement, presence of sag times and bright spots in Miocene beds).

The assumed geometry is consistent with the correlation of distinguished layers in the correlation profile P-6–P-4 (the part of this profile in the deposit zone is shown in Figure 5). The correlation profile was prepared using GeoGraphix Model Builder (*Landmark Graphics Co.*). Correlated seismo-lithological layers correspond to boundaries, which are distinctly visible on all interpreted seismic profiles in the field P (Fig. 2). The block velocity of the layers was obtained from calibrated sonic logs, VELOCITY_SONIC. In the gas horizons, apart from VELOCITY_SONIC (black blocks) VELOCITY_Q (checkered blocks) were also included.

SEISMIC MODEL — VELOCITY

The velocity curve from the acoustic log (VELOCITY_SONIC) was assumed as correct in the vicinity of the gas deposit. It was the result of detailed analysis of the acoustic log in the well P-6, in which the expected increase of transit interval time in gas horizons was not visible. The VELOCITY_Q curve, as a result of including of attenuation in process of wave propagation, was adopted in the deposit zone. This velocity corresponds to other parameters in gas horizons (Table 1).

SEISMIC MODELLING

Seismic modelling enables the correlation of seismic anomalies with their sources. In this discussed case study, 1D seismic modelling (synthetic seismograms) was applied to determine the effect of gas saturation on seismic data, whereas 2D seismic modelling (synthetic sections) was used to evaluate the seismic pattern deformation, which may be observed in zones of multi-horizon gas deposits. First, calculations were carried out for a seismogelogical model from which gas was removed (model “without gas”), then for a model representing the actual deposit (model “with gas”). Comparing the calculated theoretical wave fields one can see the scale of gas-induced seismic anomalies.

The theoretical wave field was calculated in the GeoGraphix system (*Landmark Graphics Co.*). 1D modelling was made using the LogM software, while 2D modelling was made using the STRUCT 2D:

— NORMAL INCIDENCE — synthetic section was computed based on the ray propagation theory with an assumption of ray incidence normal to seismic boundaries; it corresponds to an unmigrated seismic section after stacking but without diffraction waves,

— DIFFRACTION — synthetic section was computed based on the solution of the Hilterman wave equation, in which it is assumed that energy is dispersed in each point on the reflecting surface. The result of computing represents an unmigrated seismic section after stacking but with all diffraction waves. Generated seismic traces must be additionally migrated. The GeoGraphics system has an option with f-k migration using the Stolt method.

The signal estimated from seismic line 30-I-75K with LogM software was used in 1D and 2D modelling.

SYNTHETIC SEISMOGRAMS

Synthetic seismograms were calculated for the three velocity models given above. The seismograms are shown in Figure 6 together with the velocity curves (VELOCITY_SONIC, VELOCITY_RHG and VELOCITY_Q), GR, and the segments of seismic line 30-I-75K. Boundaries of gas horizons are marked in the figure. Comparing synthetic seismograms for models “without gas” (assuming that in the VELOCITY_SONIC there is no influence of gas) and “with gas” (assuming that in the VELOCITY_Q the influence of gas is included) one can see a distinct increase in amplitude of signals from reservoir horizons. Also, enhanced correlation between seismograms for a model “with gas” and seismic records was observed. The best correlation was obtained for a model in which VELOCITY_Q was used in modelling the theoretical wavefield (Fig. 4).

THEORETICAL WAVEFIELD — MODEL “WITHOUT GAS”

A seismogeological model named “without gas” was adopted in zones outside gas horizons. The synthetic section in these zones was constructed using velocity distribution in layers described by a VELOCITY_SONIC curve. Calculated theoretical seismic sections are shown in Figure 6a (NORMAL INCIDENCE) and in Figure 6b (REFLECTION STRENGTH). Instantaneous characteristics illustrate the bright spots in the best way (Taner and Sheriff, 1977). Comparing synthetic sections with a seismogeological model one can see that almost all boundaries are displayed in the seismic section and it is possible to correlate them along the entire line. The signal amplitudes are strictly associated with acoustic impedance contrasts at layer interfaces.

THEORETICAL WAVEFIELD — MODEL "WITH GAS"

A seismogeological model named "with gas" was adopted in gas horizons. In constructing theoretical seismic sections for this model, velocity distribution in layers was described by the VELOCITY_Q in the deposit, and by VELOCITY_SONIC curve in the other zones. The theoretical sections are shown in Figure 7a (normal) and in Figure 7 b (diffraction+Stolt migration) and in Figure 7c (normal-reflection strength).

CRITERIA FOR DETERMINATION OF RESERVOIR ZONES FROM SEISMIC SECTION INTERPRETATION

Based on both synthetic sections: "with gas" (Fig. 7) and "without gas" (Fig. 6), criteria for determining reservoir zones from seismic data interpretation may be established for gas field P. The following characteristic anomalies were observed in the deposit zone:

— A distinct increase in amplitudes of signals for reservoir layers (bright spot) in a time interval of 1000 to 1300 ms. It corresponds to a zone of major gas-bearing horizons. Beyond the deposit amplitudes are lower and their maxima are shifted in relation to the position of layers for a model "with gas". A signal amplitude change is best seen in reflection strength sections. This change may be due to lower seismic wave velocity in gas horizons.

— Small decrease in amplitude of reflections beneath the deposit series (dim spot).

— Local sag associated with longer time of seismic wave propagation in gas-bearing horizons, *e.g.* double reflection at a 1050 ms time.

— Bright spot events in zones of horizontal and synclinal arrangement of seismic boundaries.

SEISMIC DATA INTERPRETATION

Results obtained for the gas field P confirmed that criteria for determining reservoir zones from seismic data interpretation were correct. Interpretation of the 30-I-75K line made in the CHARISMA system shows how deposit P is represented in the seismic section. A part of a processed section is shown in Fig. 8a (seismic section) and in Fig. 8b (reflection strength). The following characteristics are observed in the time interval 600–1400 ms:

— bright spot for horizontally arranged seismic boundaries at a shallow depth, and for synclinally arranged seismic boundaries at a greater depth,

— local sag, *e.g.* a signal recorded at a 1050 ms.

Marked gas horizons in the lower part of seismic section (z1-z7) were confirmed by results of well log interpretations and by inflow observed in borehole P-6. Probable gas horizons (e1-e4) in the upper part of seismic section are the result of interpretation with adopted criteria. In this interval the packer measurements were not done.

A distinct decrease in signal amplitudes was observed for times greater than 1400 ms. This may be caused by enhanced attenuation of seismic waves propagating through the gas horizons. Moreover, strong, inclined reflections from the basement suddenly disappear beneath the deposit zone. These effects were not observed in theoretical sections, because no seismic wave attenuation was included in modelling. The attenuation was indirectly introduced only by decreasing the VELOCITY_Q value.

The similarity between the layer arrangement in a recorded seismic section (Fig. 8) and theoretical sections (Figs. 6 and 7) proves that the velocity model and criteria for seismic data interpretation were correctly defined. A small disagreement between recorded and theoretical wave fields may be caused by inaccurate approximation of layer arrangement by a geometric model and by inadequate identification of petrophysical parameters of the rock mass.

To correctly approximate the velocity field for a deposit with dimensions similar to those of gas field P, acoustic log data should be available from at least three boreholes in the deposit zone and beyond it. Since our studies were based on acoustic log from borehole P-6 alone and no acoustic logs were made in wells P-2 and P-4, the credibility of the model adopted is lower.

CONCLUSIONS

We show how the correct selection of elastic and reservoir parameters for Miocene sandy-shaly deposits affects the interpretation of a seismic image of a multi-horizon gas deposit. Including information about attenuation of elastic waves improves the velocity model and makes it more credible. The interpretation criteria determined in this study may be used for similar cases of gas fields in the Carpathian Foredeep.

Acknowledgements. The authors thank the Geophysical MicroComputer Application (International) Ltd. and the Schlumberger Company for use of their software in preparing this paper. The authors are also grateful to Geofizyka Kraków, Ltd. and POGC, Warsaw, for access to seismic data, logs, and geological data. Results were obtained in scientific projects No 9T12B01011 and 9T12B01517 financed by the Polish State Committee for Scientific Research.

Results were partially presented in the following conferences: 70th Annual Meeting of SEG, Calgary, 2000, Petrophysics Meets Geophysics, Paris, 2000 and Małopolska Prowincja Naftowa: Geologia i Złoża Węglowodorów, Warszawa, 2001.

REFERENCES

AKI K. and RICHARDS P. G. (1980) — Quantitative Seismology. 1. W. H. Freeman and Co.

BAŁA M. (2001) — Estimation of the influence of gas presence in the pore space on the velocity of elastic waves for the chosen layers in the well P-6. Proc. of Conf .” Nauki o Ziemi w badaniach podstawowych, złożowych i ochronie Środowiska na progu XXI wieku.” AGH, Kraków, 183–188.

BAŁA M. and JARZYNA J. (1992) — System of automatic interpretation of full waveform recorded during acoustic logging. Acta Geophys. Pol., **40**: 49–61.

BLACKBURN G. (1986) — Direct hydrocarbon detection. Some examples. Exp. Geophys., **17**: 59–66.

BORYS Z., MADEJ K., MYLŚLIWIEC M. and TRYGAR H. (1999) — Preliminary results of the new methodology of gas exploration in the northeastern part of Carpathian Foredeep. Oil and Gas News from Poland, **9**: 97–108.

DE S. G., WINTERSTEIN D. F. and MEADOWS M. A. (1994) — Comparison of P-wave and S-wave velocities and Q’s from VSP and sonic log data. Geophysics, **59**: 1512–1529.

DILAY A. J. (1982) — Direct hydrocarbon indicators lead to Canadian gas field. World Oil, **195**: 149–164

HARDAGE B. A. (1985) — Vertical seismic profiling. Handbook of Geophysical Exploration 14A. Geophys. Press

JARZYNA J. (1999) — Influence of Gas on Attenuation of Elastic Waves. In: Investigations of Seismic Anomalies and Geochemical Anomalies in Vertical Gas Migration Zones (ed. K. Pietsch *et al*.) Unpublished report in Polish of KBN project No 9T12B01011.

KARNKOWSKI P. (1999) — Oil and gas deposits in Poland. Geosynoptics Society “Geos”

KRZYWIEC P. (2001) — Contrasting tectonic and sedimentary history of the central and eastern parts of the Polish Carpathian Foredeep Basin — results of seismic data interpretation. In: The Hydrocarbon Potential of the Carpathian-Pannonian Region (eds. S. Cloetingh, M. Nemcok, F. Neubauer, F. Horvath, and P. Seifert). Marine Petrol. Geol., **18** (1): 13–38

PIETSCH K., DEREŃ D. and GĄSIOROWSKI T. (1998) — Seismic anomalies caused by multi-horizon gas deposit in north-eastern part of the Carpathian Foredeep. Prz. Geol., **46** (8): 676–684.

OSZCZYPKO N. (1996) — The Miocene dynamics of the Carpathian Foredeep in Poland. Prz. Geol., **44** (10): 1007–1018.

RAYMER L. L., HUNT E. R. and GARDNER J. S. (1980) — An improved sonic transit time to porosity. Proceedings of 21st SPWLA.

SHERIFF R. E. ed. (1992) — Reservoir Geophysics. Tulsa

STEWART R. R., HUDDLESTON P. D. and KAN T. K. (1984) — Seismic versus sonic velocities: a vertical seismic profiling study. Geophysics, **49**: 1153–1168

STUPNICKA E. (1989) — Geologia regionalna Polski. Wyd. Geol.

TANER M. T. and SHERIFF R. E. (1977) — Application of amplitude, frequency and other attributes to stratigraphic and hydrocarbon exploration. In: Seismic Stratigraphy — Application to Hydrocarbon Exploration (ed. C. E. Payton). AAPG, Memoir, **26**: 301–328.

TOVERUND T. and URSIN B. (1998) — Comparison of different seismic attenuation laws. In: Proc. of Conf. and Exhib. Modern Exploration and Improved Oil and Gas Recovery Methods, East Meets West, Kraków.